

# Pentamidine Movement across the Murine Blood-Brain and Blood-Cerebrospinal Fluid Barriers: Effect of Trypanosome Infection, Combination Therapy, P-Glycoprotein, and Multidrug Resistance-Associated Protein

Lisa Sanderson, Murat Dogruel, Jean Rodgers, Harry Pieter De Koning, and Sarah Ann Thomas

King's College London, Pharmaceutical Sciences Research Division, London, United Kingdom (L.S., M.D., S.A.T.); Division of Infection and Immunity, University of Glasgow Veterinary School, Glasgow, United Kingdom (J.R.); and Institute of Biomedical and Life Sciences, Division of Infection and Immunity, University of Glasgow, Glasgow, United Kingdom (H.P.D.K.)

Received December 16, 2008; accepted March 3, 2009

## ABSTRACT

During the first stage of human African trypanosomiasis (HAT), *Trypanosoma brucei gambiense* is found mainly in the blood, and pentamidine treatment is used. Pentamidine is predominantly ineffective once the parasites have invaded the central nervous system (CNS). This lack of efficacy is thought to be due to the inability of pentamidine to cross the blood-brain barrier, although this has never been explored directly. This study addresses this using brain perfusion in healthy mice, P-glycoprotein-deficient mice, and in a murine model of HAT (*T. brucei brucei*). The influence of additional antitrypanosomal drugs on pentamidine delivery to the CNS also was investigated. Results revealed that [<sup>3</sup>H]pentamidine can cross the blood-brain barrier, although a proportion was retained by the capillary endothelium and failed to reach the healthy or trypanosome-infected brain (up to day 21 p.i.). The CNS distribution of pentamidine

was increased in the final (possibly terminal) stage of trypanosome infection, partly because of loss of barrier integrity (days 28–35 p.i.) as measured by [<sup>14</sup>C]sucrose and [<sup>3</sup>H]suramin. Furthermore, pentamidine distribution to the CNS involved influx and efflux [via P-glycoprotein and multidrug resistance-associated protein (MRP)] transporters and was affected by the other antitrypanosomal agents, suramin, melarsoprol, and nifurtimox, but not eflornithine. These interactions could contribute to side effects or lead to the development of parasite resistance to the drugs. Thus, great care must be taken when designing drug combinations containing pentamidine or other diamidine analogs. However, coadministration of P-glycoprotein and/or MRP inhibitors with pentamidine or other diamidines might provide a means of improving efficacy against CNS stage HAT.

Human African trypanosomiasis (HAT) or sleeping sickness is fatal unless treated and is a major cause of mortality in Africa (Kennedy, 2006). After infection, the parasites initially remain in the blood and lymphatic system, and *Trypanosoma brucei rhodesiense* can be treated with suramin, and *Trypanosoma brucei gambiense* can be treated with pentamidine. Neither suramin nor pentamidine are effective against the second stage of infection, which is when the parasites become established within the CNS. This is believed to be due to their inability to cross the blood-brain barrier (BBB) (Sanderson et al., 2007), although this has not been investigated directly for pentamidine until now. Pentamidine is also used in the treatment of

American cutaneous leishmaniasis and in the treatment and prophylaxis of *Pneumocystis jirovecii* pneumonia (the cause of death of many AIDS patients). It is a diamidine, and the success of pentamidine has led to numerous diamidine compounds being developed (Sturk et al., 2004). We recently investigated the ability of the stage 1 drug, suramin, and the stage 2 drug, eflornithine, to cross the blood-brain and blood-CSF barriers in healthy and trypanosome-infected mice (Sanderson et al., 2007, 2008). As expected, suramin did not cross the blood-CNS interfaces well; however, surprisingly, eflornithine (the drug used to treat cerebral parasites) also had a limited ability to reach either healthy or infected brain. In fact, the reason eflornithine has to be administered so intensively is probably related in part to this limited CNS distribution.

Transporters are considered essential in the mode of action of pentamidine against trypanosomes and include an adeno-

This work was supported by The Wellcome Trust [Grants 073542, 080268]. Article, publication date, and citation information can be found at <http://jpet.aspetjournals.org>. doi:10.1124/jpet.108.149872.

**ABBREVIATIONS:** HAT, human African trypanosomiasis; CNS, central nervous system; BBB, blood-brain barrier; CSF, cerebrospinal fluid; P-gp, P-glycoprotein; MRP, multidrug resistance-associated protein; CVO, circumventricular organ; DMSO, dimethyl sulfoxide; p.i., postinfection; HPLC, high-performance liquid chromatography.

sine-sensitive pentamidine transporter (or P2), an adenosine-insensitive high-affinity pentamidine transporter 1, and an adenosine-insensitive low-affinity pentamidine transporter 1 (de Koning, 2001). Pentamidine transporters have also been demonstrated in certain *Leishmania* species (Basselin et al., 2002), including P-glycoprotein (P-gp)-like (Leprohon et al., 2006) and multidrug resistance-associated protein (MRP)-like (pentamidine resistance protein 1) transporters (Coelho et al., 2003). Because pentamidine interacts with multiple parasitic transporters (Bridges et al., 2007), its penetration into the CNS could likewise be aided by transporters (e.g., nucleoside/nucleobase transporters) or restricted by transporters (e.g., P-glycoprotein/MRP) expressed at the blood-CNS barriers. Potential drug interactions with transporters expressed at these barrier interfaces are of special significance because of the interest in optimizing drug therapy and reducing toxicity by administering antitrypanosomal drugs in parallel (Priotto et al., 2007). It is already known that pentamidine and other antitrypanosomal drugs can interact at the level of the transporter because loss of trypanosome transporters are well established as causing the cross-resistance between pentamidine and the stage 2 drug, melarsoprol (Bridges et al., 2007). A thorough investigation of how pentamidine crosses the blood-CNS barriers and how it interacts with mammalian transporters is warranted not only to aid the development of new drugs with enhanced CNS efficacy but also to select effective drug combination therapies (i.e., pentamidine in combination with suramin, eflornithine, melarsoprol, or nifurtimox) and is the main objective of this study.

We examined the CNS distribution of pentamidine, by means of a sensitive brain/choroid plexus perfusion technique in wild-type and P-gp-deficient mice (Sanderson et al., 2007). By means of this perfusion technique, we also investigated the interaction of pentamidine with MRP, nucleoside, and nucleobase transporters. The effect of combining pentamidine with other antitrypanosomal drugs (e.g., suramin, eflornithine, melarsoprol, and nifurtimox) was also examined. In addition, we combined the brain perfusion technique with a murine model of HAT (Sanderson et al., 2008), which permitted an evaluation of pentamidine CNS distribution during the course of trypanosome infection. The function of the neural barriers in disease has been classified recently as a high-priority research area to improve the success rate of drugs developed to treat CNS disorders (Neuwelt et al., 2008).

## Materials and Methods

**Materials.** Pentamidine (1,5-bis-4'-amidinophenoxy)pentane isethionate salt (mol. wt., 592.68; 98% purity) was purchased from Sigma Chemical (Poole, Dorset, UK). [<sup>3</sup>H(G)]pentamidine (mol. wt., 340.4; specific activity, 5 Ci/mmol; 99% radiochemical purity) was synthesized and tritiated (Moravek Biochemicals, Brea, CA). [<sup>14</sup>C]sucrose (498 mCi/mmol) and [<sup>3</sup>H]suramin sodium (5.1–6.2 Ci/mmol) were purchased from Moravek Biochemicals. Eflornithine (DL- $\alpha$ -difluoromethylornithine; mol. wt., 237) is administered clinically as a racemate, although the L-enantiomer is the active moiety (Burri and Brun, 2003). D-Eflornithine and L-eflornithine hydrochloride were a gift of Genzyme (Cambridge, MA). Eflornithine hydrochloride and suramin sodium salt were purchased from Sigma Chemical and Calbiochem (San Diego, CA), respectively. Nifurtimox [N-(3-methyl-1,1-dioxo-1,4-thiazinan-4-yl)-1-(5-nitro-2-furyl)methanimine] and melarsoprol [(2-(4-(4,6-diamino-1,3,5-triazin-2-ylamino)-phenyl)-1,3,2-dithiarsolan-4-yl)methanol] were a kind gift from Pro-

fessor Simon Croft (London School of Hygiene and Tropical Medicine, London, UK).

**Animals.** All procedures were performed within the guidelines of the Animal Scientific Procedures Act (1986) and Animal Pathogen Order (1998; UK). BALB/c mice were purchased from Harlan UK Limited (Bicester, Oxon, UK). FVB-Mdr1a/1b(+/+) and FVB-Mdr1a/1b(-/-) mice were imported from Taconic Farms (Germantown, NY) and a breeding colony established at King's College London under an academic breeding agreement. Dr. Alfred Schinkel of the Netherlands Cancer Institute is the creator of Mdr1a/1b mice. CF-1 mdr1a(+/+) mice and CrI:CF1-mdr1a(-/-) mice were obtained from Charles River (Margate, Kent, UK). All animals were maintained under standard temperature/lighting conditions and given food and water ad libitum.

**Perfusion Technique.** The brain was perfused via a cannula placed in the heart as described previously (Sanderson et al., 2007). Adult male mice (~25 g) were anesthetized (2 mg/kg i.p. medetomidine hydrochloride and 150 mg/kg i.p. ketamine) and heparinized (100 U i.p.). The left ventricle of the heart was cannulated and perfused (5 ml/min) with an oxygenated artificial plasma for up to 30 min. The right atrium was sectioned. At the end of this time, a cisterna magna CSF sample was taken, and the brain was removed. Samples of the frontal cortex, occipital cortex, caudate putamen, hippocampus, hypothalamus, thalamus, pons, cerebellum, fourth ventricle choroid plexus, and pineal and pituitary glands were taken under a Leica S4 E stereozoom microscope (Leica, Wetzlar, Germany). These regions were selected to determine drug concentration in areas affected by the trypanosome (Sanderson et al., 2007). All of the brain matter remaining after these regions had been taken underwent capillary depletion analysis as described previously (Sanderson et al., 2008). This involved the preparation of a brain homogenate and a dextran-density gradient centrifugation step to produce an endothelial cell enriched pellet and a brain parenchyma-containing supernatant. Capillary depletion (including brain homogenate, supernatant, and pellet), brain regions, circumventricular organs (CVOs; i.e., choroid plexus, pituitary and pineal glands), plasma, and CSF samples were solubilized with 0.5 ml of Solvable (PerkinElmer Life and Analytical Sciences, Waltham, MA). Liquid scintillation fluid (3.5 ml; Lumasafe; PerkinElmer Life and Analytical Sciences) was then added. Sample radioactivity was counted using a Packard Tri-Carb2900TR scintillation counter with ultralow-level count mode software.

**Multiple-Time Experiments.** Brain perfusions were performed, as described above, in BALB/c mice. [<sup>3</sup>H]Pentamidine (0.1  $\mu$ M) and [<sup>14</sup>C]sucrose (1.0  $\mu$ M) were infused into the plasma via a syringe pump for 2.5 to 30 min. [<sup>14</sup>C]sucrose is not able to cross cell membranes. Hence, it is used as a vascular space marker in the brain samples and increases in its value indicates loss of BBB integrity. In the pineal and pituitary gland samples, [<sup>14</sup>C]sucrose values represent the vascular space and reflect the ability of [<sup>14</sup>C]sucrose to cross between the capillary endothelial cells in the absence of tight junctions. Thus, [<sup>14</sup>C]sucrose also provides a measure of the paracellular permeability characteristics of these tissues. In choroid plexus samples, [<sup>14</sup>C]sucrose represents the vascular space and extracellular space formed between the choroidal capillary endothelium and epithelium.

**Drug Combination Experiments.** Ten-minute perfusions were also performed using BALB/c mice and [<sup>3</sup>H]pentamidine (0.1  $\mu$ M) and [<sup>14</sup>C]sucrose (1.0  $\mu$ M) plus unlabeled 10  $\mu$ M pentamidine (Waalkes and DeVita, 1970), 100  $\mu$ M pentamidine, 150  $\mu$ M suramin, 250  $\mu$ M eflornithine (Milord et al., 1993), 30  $\mu$ M melarsoprol, or 15  $\mu$ M nifurtimox (González-Martin et al., 1992). Further experiments explored the effect of 100  $\mu$ M adenine or 100  $\mu$ M adenosine (Murakami et al., 2005) on [<sup>3</sup>H]pentamidine CNS uptake (10 min). Unlabeled pentamidine, melarsoprol, and nifurtimox required dissolution in DMSO. The final DMSO concentration in the plasma was 0.05%. Control groups were provided by [<sup>3</sup>H]pentamidine and [<sup>14</sup>C]sucrose distribution being examined in the presence of 0.05% DMSO.

**P-Glycoprotein and MRP Transport.** P-gp is an efflux transporter expressed at the human and murine BBB (Cordon-Cardo et al., 1989; Soontornmalai et al., 2006) and hypothesized to contribute to the synergism effect of antitrypanosomal drugs when they are used in combination. In humans, the drug-transporting P-gp isoform is MDR1, and in rodents, it is *mdr1a* and *mdr1b* (Borst and Schinkel, 1997). Although the homology of *mdr1a* and *mdr1b* is similar, it is not exact; therefore, there is a possibility that substrates and inhibitors may bind to the isoforms differently. In the present study, we used knockout mice with disruptions of the *Mdr1a* gene and mice with disruptions of both *Mdr1a* and *Mdr1b* genes. FVB-Mdr1a/Mdr1b(+/+) and FVB-Mdr1a/Mdr1b(-/-) mice were perfused for 30 min with [<sup>3</sup>H]pentamidine and [<sup>14</sup>C]sucrose. This was then repeated using CF1-mdr1a(+/+) and CF1-mdr1a(-/-) mice.

Further experiments using [<sup>3</sup>H]pentamidine and [<sup>14</sup>C]sucrose and 100  $\mu$ M unlabeled pentamidine (0.05% DMSO) were performed in FVB-Mdr1a/Mdr1b(-/-) mice (30 min). Results were compared with those obtained from FVB-Mdr1a/Mdr1b(-/-) mice, which were perfused with [<sup>3</sup>H]pentamidine and [<sup>14</sup>C]sucrose (0.05% DMSO). Experiments were also performed in FVB-Mdr1a/Mdr1b(-/-) using 10  $\mu$ M indomethacin (in 0.05% DMSO), an inhibitor commonly used to inhibit MRP (Huai-Yun et al., 1998) but also able to inhibit other transporters (e.g., organic anion transporter 2).

**Murine Model of HAT.** The heart perfusion technique was used to examine the effects of disease on [<sup>3</sup>H]pentamidine distribution by means of a mouse model of HAT. This model, which uses cloned stabilates of *T. brucei brucei* GVR 35 to infect BALB/c mice, has been characterized (Sanderson et al., 2008). One intraperitoneal injection of  $2 \times 10^4$  trypanosomes (*T. brucei brucei* GVR 35/C1.7) diluted in 0.1 ml of phosphate-buffered saline containing glucose, pH 8.0, was used (Sanderson et al., 2008), and parasitemia was monitored in venous blood. In BALB/c mice, the CNS stage of the disease is reached at  $\sim$ day 11 postinfection (p.i.), and the average survival time is  $37.9 \pm 1.2$  days (Sanderson et al., 2008). At day 7, 14, 21, 28, and 35 p.i., individual groups of six to seven animals were in situ perfused with [<sup>3</sup>H]pentamidine (0.1  $\mu$ M) and [<sup>14</sup>C]sucrose (1  $\mu$ M) for 30 min. Day 35 p.i. mice were also in situ perfused with [<sup>3</sup>H]suramin (0.2  $\mu$ M) and [<sup>14</sup>C]sucrose (1.0  $\mu$ M) for 30 min ( $n = 4$ ). Brain samples were taken as described above.

**Expression of Results.** The amount of radioactivity in the tissue sample (disintegrations per minute per gram) was expressed as a percentage of that in the artificial plasma (disintegrations per minute per milliliter) and termed  $R_{\text{Tissue}}$  (milliliters per 100 g). Where stated, the  $R_{\text{Tissue}}$  for [<sup>3</sup>H]drug has been corrected for vascular/extracellular space by subtraction of the [<sup>14</sup>C]sucrose  $R_{\text{Tissue}}$  value. The unidirectional transfer constants ( $K_{\text{in}}$ ) and the initial volume of distribution of the test solute in the rapidly equilibrating space ( $V_i$ ), which may include the vascular space, the capillary endothelial volume, and/or compartments in parallel with the BBB, were determined by least-squares linear regression analysis of the multiple-time uptake data as described previously (Williams et al., 1996).  $K_{\text{in}}$  and  $V_i$  represent the slope of the line and ordinate intercept, respectively.

**Data Analysis.** Samples were grouped into brain parenchyma, capillary depletion, or CVOs and analyzed by two-way analysis of variance using Sigma Stat software (SPSS Inc., Chicago, IL). Where a significant difference was observed ( $P < 0.05$ ) individual region/sample comparisons were made using Tukey's pairwise comparisons. Means, S.E. values, and  $P$  values are provided as summary statistics.

**HPLC.** To monitor the integrity of the [<sup>3</sup>H]pentamidine during perfusion through the cerebral circulation, samples of the arterial inflow (i.e., drug in artificial plasma) and the venous outflow, during the last minute of a 30-min perfusion, were collected. The brains were also sampled ( $n = 3$ ). Three hundred-microliter aliquots of the plasma samples were extracted by vortexing in acetonitrile followed by centrifugation at 13,000g (4°C) for 5 min. Five hundred microliters of each of the resulting supernatants were combined and dried under  $N_2$ . Three hundred-microliter aliquots of pentamidine stan-

dards (0.5  $\mu$ M) prepared in artificial plasma were also extracted and dried as above. Brain samples were homogenized in ice-cold 10% trifluoroacetic acid (3 ml/g). Homogenates were centrifuged at 13,800g (20 min), and the supernatants were mixed with an equal volume of ether. Samples were recentrifuged at 330g (4°C) for 20 min. The lower organic phase for each of the three extracted brains were combined, dried under  $N_2$ , and redissolved in 100  $\mu$ l of 3% acetonitrile containing 10 mM heptane sulfonate, 10 mM tetramethylammonium chloride, and 4.2 mM  $H_3PO_4$ , then injected onto a Zorbax RX-C8, 5- $\mu$ ,  $4.6 \times 250$ -mm column (Berger et al., 1991). Separation was carried out by gradient elution on an HPLC system (Jasco, Tokyo, Japan). Sample elution involved using a gradient of 3.5 to 45% acetonitrile in water (1 ml/min) over 30 min. Conditions were returned to 3.5% acetonitrile over 2 min and held to allow the column to equilibrate for 3 min (35-min total time). The gradient was achieved by mixing solvents A ( $H_2O$ ) and B (50% acetonitrile), both of which contained 10 mM heptane sulfonate, 10 mM tetramethylammonium chloride, and 4.2 mM  $H_3PO_4$ . UV absorbance was monitored at 265 nm, and then the column eluant was passed into a radioactive detector (Packard, Waltham, MA), where it was mixed 1:3 with scintillation fluid (UltimaFlo M; Packard) for real-time radioactive analysis. A single peak, with a retention time of 26.5 min, was detected in the brain after 30 min with [<sup>3</sup>H]pentamidine. This retention time corresponded with that of the [<sup>3</sup>H]pentamidine standards. Chromatograms obtained from the venous outflow samples were identical to those obtained from the arterial inflow (data not shown).

**Octanol-Saline Partition Coefficient and Protein Binding.** The lipophilicity of [<sup>3</sup>H]pentamidine (0.7  $\mu$ M) was measured in the form of an octanol-saline partition coefficient, pH 7.4, and was  $0.14368 \pm 0.00337$ . Binding of [<sup>3</sup>H]pentamidine (0.7  $\mu$ M) to the colloid in the artificial plasma was determined using Centrifree micropartition devices (Millipore Corporation, Billerica, MA) and was found to be  $41 \pm 5\%$ . Further studies explored the ability of [<sup>3</sup>H]pentamidine to bind to murine (male FVB) and human (Sigma Chemical) plasma proteins. Lyophilized human plasma was reconstituted in 1 ml of deionized water. Both methods were carried out as described previously (Sanderson et al., 2007). Protein binding of [<sup>3</sup>H]pentamidine was more extensive in mouse than human plasma, with  $90 \pm 5$  and  $78 \pm 0.3\%$  being bound, respectively.

## Results

**Multiple-Time Perfusion Studies.** No differences were observed in the [<sup>14</sup>C]sucrose/vascular spaces in the frontal cortex, caudate putamen, occipital cortex, hippocampus, hypothalamus, and thalamus over time, and at 30 min, values ranged from 1.6% (hippocampus) to 2.8% (hypothalamus). The vascular spaces measured in the cerebellum and the pons over time were higher than in the other brain regions ( $P < 0.001$ ), and at 30 min, values were  $3.2 \pm 0.4$  and  $3.7 \pm 0.6\%$ , respectively (Fig. 1). [<sup>14</sup>C]Sucrose distribution into the brain over time was not linear.

[<sup>3</sup>H]pentamidine  $R_{\text{Tissue}}$  values were higher than those for the vascular space in all brain regions ( $P < 0.001$ ; Fig. 1). [<sup>3</sup>H]Pentamidine distribution ([<sup>14</sup>C]sucrose-corrected) into the brain over time could be described by a linear relationship. Thus, multiple-time uptake analysis was used to determine  $K_{\text{in}}$  and  $V_i$  (Fig. 1). The levels of [<sup>3</sup>H]pentamidine ([<sup>14</sup>C]sucrose-corrected) in the pons were higher than those detected in the other brain regions at all time points ( $P < 0.001$ ).

The [<sup>14</sup>C]sucrose-corrected  $R_{\text{Tissue}}$  values for [<sup>3</sup>H]pentamidine in the choroid plexus and pineal and pituitary glands reached  $1275 \pm 109$ ,  $465 \pm 117$ , and  $301 \pm 34$  ml/100 g, respectively, after 30 min. All the values obtained over time

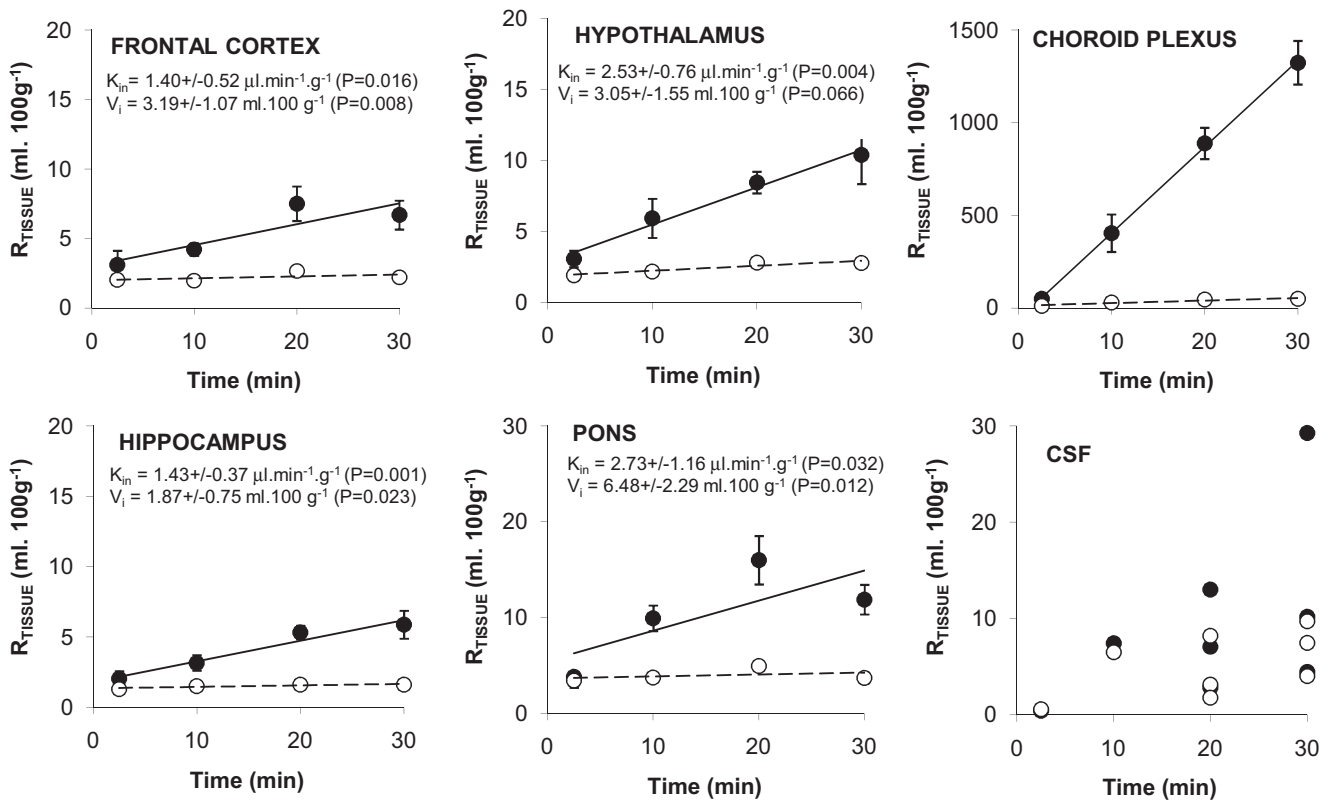


**Fig. 1.** Percentage of  $[^3\text{H}]$ pentamidine (—●—) and  $[^{14}\text{C}]$ sucrose (—○—) detected in samples relative to that in the plasma ( $R_{\text{Tissue}}$ ) versus times. Each data point represents  $n = 3$  to 6, except for CSF, where individual points are plotted because of the limited number of samples obtained. The slopes ( $K_{\text{in}}$ ) and intercepts of the curves ( $V_i$ ) for  $[^3\text{H}]$ pentamidine distribution into the brain were determined.

were above those for  $[^{14}\text{C}]$ sucrose ( $P < 0.001$  for each organ) (Fig. 1). The  $R_{\text{Tissue}}$  values for  $[^3\text{H}]$ pentamidine and  $[^{14}\text{C}]$ sucrose into the CSF were  $7.6 \pm 3.0$  and  $4.4 \pm 3.4$  ml/100 g, respectively, after a 20-min perfusion ( $n = 3$ ; Fig. 1).

$[^3\text{H}]$ Pentamidine was detected at higher levels than  $[^{14}\text{C}]$ sucrose in the homogenate, supernatant, and the endothelial cell-enriched pellet ( $P < 0.001$  for each sample). The  $[^3\text{H}]$ pentamidine  $R_{\text{Tissue}}$  value ( $[^{14}\text{C}]$ sucrose-corrected) in the homogenate after a 30-min perfusion was  $5.4 \pm 1.3$  ml/100 g, but after capillary depletion analysis, the pellet had a value of  $15.1 \pm 2.4$  ml/100 g, and the supernatant had a value of  $2.0 \pm 0.4$  ml/100 g (Fig. 2). The large pellet accumulation explains the differences between the  $V_i$  values achieved for  $[^3\text{H}]$ pentamidine (Fig. 1) and those previously obtained for  $[^{14}\text{C}]$ sucrose,  $1.66 \pm 0.15$  ml/100 g (Williams et al., 1996).

**Saturation Studies.** DMSO had no effect on the  $R_{\text{Tissue}}$  for  $[^{14}\text{C}]$ sucrose or  $[^3\text{H}]$ pentamidine in the brain, CVOs, or capillary depletion samples ( $P > 0.05$  for each molecule for each tissue group). Likewise, unlabeled pentamidine had no effect on vascular/ $[^{14}\text{C}]$ sucrose space compared with the addition of 0.05% DMSO alone ( $P > 0.05$  for brain, capillary depletion samples, and CVOs, respectively). However, the addition of 10 or 100  $\mu\text{M}$  unlabeled pentamidine increased the sucrose-corrected brain uptake of  $[^3\text{H}]$ pentamidine in a dose-dependent manner ( $P < 0.001$  for DMSO versus 100  $\mu\text{M}$ ,  $P < 0.001$  for 100 versus 10  $\mu\text{M}$ , and  $P = 0.010$  for 10  $\mu\text{M}$  compared with DMSO controls; Fig. 3). For the 10  $\mu\text{M}$  concentration, the  $[^{14}\text{C}]$ sucrose-corrected  $[^3\text{H}]$ pentamidine values ranged from 0.95 to 2.2 times those of the DMSO controls. For the 100  $\mu\text{M}$  concentration, the  $[^{14}\text{C}]$ sucrose-

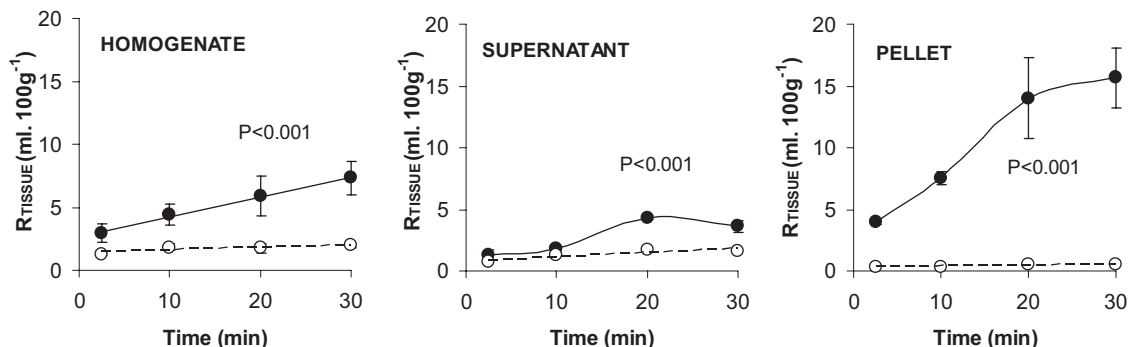


**Fig. 2.** Percentage of  $[^3\text{H}]$ pentamidine (—●—) and  $[^{14}\text{C}]$ sucrose (—○—) detected in the homogenate, supernatant, and pellet relative to that in the plasma ( $R_{\text{Tissue}}$ ) after capillary depletion analysis of the brain homogenate at various perfusion times. Each data point represents  $n = 3$  to 6. Two-way analysis of variance was used to compare  $[^3\text{H}]$ pentamidine and  $[^{14}\text{C}]$ sucrose values, and statistical significance is reported.

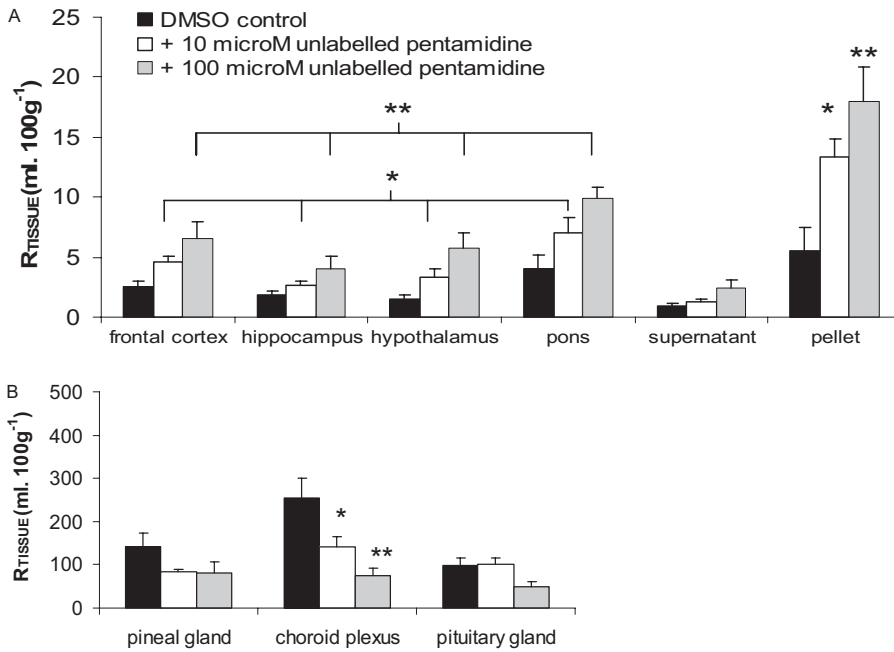


**Fig. 3.** [<sup>14</sup>C]Sucrose-corrected uptake of [<sup>3</sup>H]pentamidine in the brain parenchyma and the supernatant and pellet samples achieved after capillary depletion analysis of the brain homogenate (A) and CVOs of mice perfused for 10 min with artificial plasma containing either 10 or 100  $\mu$ M unlabeled pentamidine in DMSO, compared with DMSO alone (B). Each data point represents  $n = 3$  to 5. \*,  $P \leq 0.01$ ; \*\*,  $P < 0.001$  compared with DMSO control.

corrected [<sup>3</sup>H]pentamidine values ranged from 1.8 to 3.8 times those of the DMSO controls. Capillary depletion analysis revealed that unlabeled pentamidine also resulted in a dose-dependent increase in [<sup>3</sup>H]pentamidine uptake into the capillary endothelial cell-enriched pellet ( $P < 0.001$  for 100  $\mu$ M pentamidine versus DMSO control,  $P = 0.007$  for 10  $\mu$ M versus DMSO control and  $P < 0.001$  for 10 versus 100  $\mu$ M), but there was no statistically significant increase into the supernatant at either concentration (Fig. 3). Unlabeled pentamidine caused a decrease in the sucrose-corrected uptake of [<sup>3</sup>H]pentamidine into the CVOs, and this attained significance in the choroid plexus, where 10 and 100  $\mu$ M unlabeled pentamidine resulted in a 44 ( $P = 0.006$ ) and 70% ( $P < 0.001$ ) decrease, respectively. The decreases observed in the pineal

and pituitary glands did not attain statistical significance (Fig. 3).

**[<sup>3</sup>H]Pentamidine Efflux by P-Glycoprotein as Expressed by *mdr1a/mdr1b* (FVB).** No differences were observed in the vascular/[<sup>14</sup>C]sucrose space detected in brain, CVOs, or capillary depletion analysis samples ( $P > 0.05$ , respectively) taken from FVB-*mdr1a/1b*(-/-) compared with FVB-*mdr1a/1b*(+/+) mice. In contrast, the distribution of sucrose-corrected [<sup>3</sup>H]pentamidine was 2 to 3 times higher (or increased by 103–219%) in the brain regions sampled from the FVB-*mdr1a/1b*(-/-), compared with those in the wild-type mice ( $P < 0.001$ ; Fig. 4A). This increase in accumulation was also observed in the capillary depletion samples ( $P = 0.006$ ; Fig. 4A). No differences were observed in the

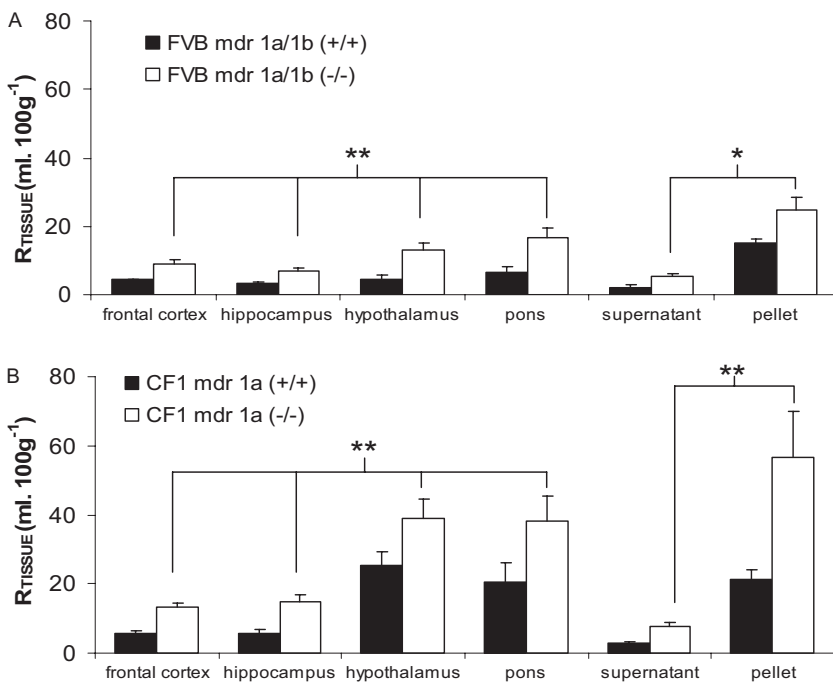


**Fig. 4.** [<sup>14</sup>C]Sucrose-corrected uptake of [<sup>3</sup>H]pentamidine in brain regions and capillary depletion samples of FVB-*mdr 1a/1b*(+/+) compared with FVB-*mdr 1a/1b*(-/-) mice (A) and CF-1 *mdr1a*(+/+) compared with CF-1 *mdr1a*(-/-) mice (B). Perfusion time, 30-min perfusion. Each data point represents  $n = 5$  to 12. \*,  $P < 0.01$ ; \*\*,  $P \leq 0.001$  compared with wild-type strains.

sucrose-corrected uptake of [ $^3\text{H}$ ]pentamidine into the CVOs between the FVB-*mdr1a/1b*( $-/-$ ) and FVB-*mdr1a/1b*( $+/+$ ) mice.

**[ $^3\text{H}$ ]Pentamidine Efflux by P-Glycoprotein as Expressed by *mdr1a* (CF-1).** Similar trends to the FVB strains were observed between the CF1-*mdr1a*( $-/-$ ) and CF1-*mdr1a*( $+/+$ ) strains (Fig. 4B). No differences were observed in the [ $^{14}\text{C}$ ]sucrose space in brain, CVOs, or capillary depletion samples taken from the CF1-*mdr1a*( $-/-$ ) mice compared with CF1-*mdr1a*( $+/+$ ) controls. However, the distribution of [ $^3\text{H}$ ]pentamidine ([ $^{14}\text{C}$ ]sucrose-corrected) was 1.5 to 3 times higher (or increased by 54–205%) in the brain ( $P < 0.001$ ) and capillary depletion samples ( $P = 0.001$ ) taken from the CF1-*mdr1a*( $-/-$ ) mice compared with the wild-type mice (Fig. 4B). No differences were observed in the [ $^{14}\text{C}$ ]sucrose-corrected uptake of [ $^3\text{H}$ ]pentamidine into the CVOs between the CF1-*mdr1a*( $-/-$ ) compared with the CF1-*mdr1a*( $+/+$ ) mice ( $P = 0.105$ ).

**Comparison of FVB and CF-1 Mice Strains.** Vascular space as measured by [ $^{14}\text{C}$ ]sucrose was 1.7 times higher in the hypothalamus ( $P = 0.003$ ) and 1.8 times higher in the pons ( $P < 0.001$ ) of CF1 compared with FVB wild-type mice. However, the vascular space in the other brain regions was similar in both strains ( $P > 0.05$  for each region). Likewise, no significant differences were observed between strains in the [ $^{14}\text{C}$ ]sucrose spaces measured in the capillary depletion samples ( $P = 0.866$ ) and the CVOs ( $P = 0.876$ ).

The [ $^{14}\text{C}$ ]sucrose-corrected uptake of pentamidine was 6 times higher in the hypothalamus ( $P < 0.001$ ) and 3 times higher in the pons ( $P < 0.001$ ) of CF1 compared with FVB wild-type mice, whereas no significant differences were observed in the other brain regions. [ $^3\text{H}$ ]Pentamidine distribution ([ $^{14}\text{C}$ ]sucrose-corrected) was increased by 24% in the supernatant and 42% in the pellet obtained from capillary depletion analysis of brain tissue taken from CF1 compared with FVB wild-type mice ( $P = 0.0027$ ). No differences were observed in uptake ([ $^{14}\text{C}$ ]sucrose corrected) into the CVOs ( $P = 0.763$ ).

Vascular/[ $^{14}\text{C}$ ]sucrose space was also 1.6 times higher in both the hypothalamus ( $P < 0.001$ ) and pons ( $P < 0.001$ ) of CF1-*mdr1a*( $-/-$ ) compared with FVB-*mdr1a/1b*( $-/-$ ) mice. However, in the other brain regions, measurements for vascular space were similar in both strains, and no differences were observed between strains in the vascular/[ $^{14}\text{C}$ ]sucrose spaces measured in the capillary depletion samples ( $P = 0.346$ ) and the CVOs ( $P = 0.430$ ).

In contrast, the [ $^{14}\text{C}$ ]sucrose-corrected uptake of pentamidine into brain parenchyma was 1.5 to 3.0 times higher in CF1-*mdr1a*( $-/-$ ) compared with FVB-*mdr1a/1b*( $-/-$ ) mice, depending on the region, and this was statistically significant in the occipital cortex ( $P = 0.047$ ), hippocampus ( $P = 0.028$ ), hypothalamus ( $P < 0.001$ ), thalamus ( $P < 0.001$ ), pons ( $P < 0.001$ ), and cerebellum ( $P < 0.001$ ). The [ $^{14}\text{C}$ ]sucrose-corrected uptake of pentamidine was also 2.3 times higher in the pellet of CF1-*mdr1a*( $-/-$ ) compared with FVB-*mdr1a/1b*( $-/-$ ) mice ( $P < 0.001$ ), but no difference was observed in the homogenate and supernatant ( $P > 0.05$ ) or in the CVOs ( $P = 0.298$ ).

**Additional Efflux Transporters for Pentamidine.** To study the CNS distribution of [ $^3\text{H}$ ]pentamidine in the absence of P-gp efflux, we measured [ $^3\text{H}$ ]pentamidine accumulation in FVB-*mdr1a/1b*( $-/-$ ) mice in the presence of 100  $\mu\text{M}$

pentamidine (Fig. 5). No differences were observed in [ $^{14}\text{C}$ ]sucrose or the sucrose-corrected uptake of [ $^3\text{H}$ ]pentamidine in the capillary depletion samples and CVOs from mice that were perfused with 0.05% DMSO compared with control FVB-*mdr1a/1b*( $-/-$ ) mice ( $P > 0.05$  for each isotope). Furthermore, unlabeled pentamidine (and indomethacin) had no effect on barrier integrity, as measured by [ $^{14}\text{C}$ ]sucrose space, compared with DMSO controls in the capillary depletion and CVOs sampled. However, there was an increase in the sucrose-corrected uptake of [ $^3\text{H}$ ]pentamidine in the homogenate (68%), supernatant (117%), and capillary endothelial cell-enriched pellet (58%) of the P-gp knockout mice when 100  $\mu\text{M}$  unlabeled pentamidine in 0.05% DMSO was added to the artificial plasma and compared with knockout mice that were perfused with 0.05% DMSO ( $P = 0.034$ ). In contrast, there was no difference in the sucrose-corrected [ $^3\text{H}$ ]pentamidine uptake into the CVOs between the groups. Although there was a decrease in the accumulation of [ $^3\text{H}$ ]pentamidine in the choroid plexus because of the presence of unlabeled pentamidine, this failed to attain significance (Fig. 5).

In separate experiments, indomethacin was added to the plasma, and FVB-*mdr1a/1b*( $-/-$ ) mice were perfused. An increase in the sucrose-corrected uptake of [ $^3\text{H}$ ]pentamidine was observed in the capillary depletion samples (45, 25, and 34% in the homogenate, supernatant, and pellet), respectively, when these results were compared with control FVB-*mdr1a/1b*( $-/-$ ) mice, but this was not statistically significant ( $P = 0.361$ ). However, [ $^3\text{H}$ ]pentamidine (sucrose-corrected) uptake was increased in the CVOs that were perfused with indomethacin compared with mice that were perfused with either 0.05% DMSO ( $P = 0.003$ ) or 100  $\mu\text{M}$  unlabeled pentamidine ( $P < 0.001$ ) (Fig. 5).

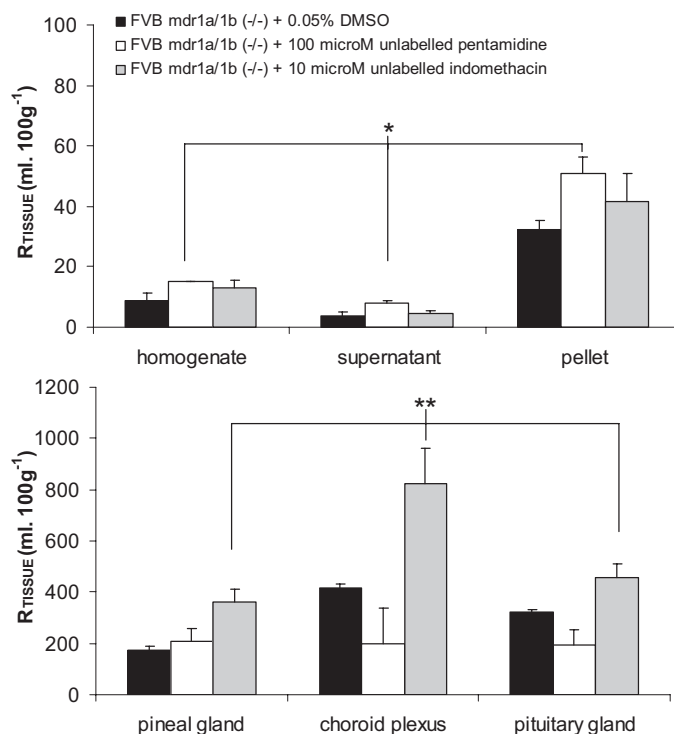


**Fig. 5.** The effect of 100  $\mu\text{M}$  unlabeled pentamidine or 10  $\mu\text{M}$  indomethacin on the [ $^{14}\text{C}$ ]sucrose-corrected uptake of [ $^3\text{H}$ ]pentamidine in FVB-*mdr1a/1b*( $-/-$ ) mice. All experiments contained DMSO, including the control group. Each group represents  $n = 5$  to 6. \*,  $P < 0.05$ ; \*\*,  $P < 0.01$  compared with controls.

**Effect of Adenosine and Adenine on [ $^3\text{H}$ ]Pentamidine Distribution.** The sucrose-corrected distribution of [ $^3\text{H}$ ]pentamidine that was measured in the brains after perfusion with 100  $\mu\text{M}$  adenosine was up to 2.6 times higher than that measured in mice that were perfused with [ $^3\text{H}$ ]pentamidine and [ $^{14}\text{C}$ ]sucrose alone ( $P < 0.001$ ). A similar increase in [ $^3\text{H}$ ]pentamidine uptake was observed in the supernatant and the capillary endothelial cell-enriched pellet from mice that were copperfused with 100  $\mu\text{M}$  adenosine ( $P = 0.019$ ; Fig. 6). No difference was observed in [ $^3\text{H}$ ]pentamidine or [ $^{14}\text{C}$ ]sucrose values in the presence of adenosine into the CVOs ( $P = 0.111$ ) ( $P > 0.05$  for brain, capillary depletion samples, and CVOs).

No differences were observed in the sucrose-corrected uptake of [ $^3\text{H}$ ]pentamidine into the brain, capillary depletion samples, or the CVOs of BALB/c mice when 100  $\mu\text{M}$  adenine was added to the artificial plasma ( $P > 0.05$  for brain, capillary depletion samples, and CVOs; Fig. 6). There was a small, but significant, decrease in vascular/[ $^{14}\text{C}$ ]sucrose space in the brain samples taken from these mice, compared with those that were perfused with 100  $\mu\text{M}$  adenosine or artificial plasma alone ( $P < 0.001$ ), but this was not observed in the capillary depletion samples or the CVOs ( $P > 0.05$ , respectively).

**Effect of Drug Combinations on [ $^3\text{H}$ ]Pentamidine Uptake.** At the concentrations used, suramin, melarsoprol, nifurtimox, or eflornithine (racemic mixture, D- or L-isomer) did not have any effect on the integrity of the blood-brain or blood-CSF barriers as measured by [ $^{14}\text{C}$ ]sucrose ( $P > 0.05$  for all samples taken from mice perfused with each of the unlabeled drugs and compared with control mice that were perfused with either plasma alone or with 0.05% DMSO).

Overall, the addition of suramin to the [ $^3\text{H}$ ]pentamidine and [ $^{14}\text{C}$ ]sucrose resulted in an 18 to 47% decrease in the sucrose-corrected uptake of [ $^3\text{H}$ ]pentamidine into the brain ( $P = 0.004$ ; Fig. 7). [ $^3\text{H}$ ]Pentamidine uptake was also decreased in the capillary depletion samples from mice that

were copperfused with suramin ( $P = 0.018$ ). This was most evident in the endothelial cell-enriched pellet where uptake decreased by 18% compared with only 4% for the supernatant. No differences were observed in the uptake of [ $^3\text{H}$ ]pentamidine into the CVOs with or without the addition of suramin to the artificial plasma.

To investigate the effect of melarsoprol and nifurtimox on the sucrose-corrected uptake of [ $^3\text{H}$ ]pentamidine, these unlabeled drugs required dissolution in 0.05% DMSO, which itself (as previously stated) had no effect on either the integrity of the barriers or the uptake of [ $^3\text{H}$ ]pentamidine. Melarsoprol caused a significant decrease in the overall brain uptake of [ $^3\text{H}$ ]pentamidine compared with control mice perfused with 0.05% DMSO ( $P = 0.002$ ; Fig. 7). Statistical significance was not obtained in the capillary depletion samples ( $P = 0.791$ ) or the CVOs ( $P = 0.832$ ) at this melarsoprol concentration.

The addition of nifurtimox resulted in an increase in the uptake of [ $^3\text{H}$ ]pentamidine into the brain ( $P < 0.001$ ; Fig. 7). This was most apparent in the hypothalamus, where [ $^3\text{H}$ ]pentamidine uptake was 5 times greater than that detected in control mice perfused with 0.05% DMSO. After capillary depletion analysis, [ $^3\text{H}$ ]pentamidine uptake was also two to three times greater in both the supernatant and capillary endothelial cell-enriched pellet obtained from mice perfused with nifurtimox compared with those obtained from control mice, but this increase only reached significance in the pellet ( $P < 0.001$ ). No differences were observed in [ $^3\text{H}$ ]pentamidine uptake into the CVOs with nifurtimox ( $P > 0.05$ ).

Eflornithine had no effect on the CNS distribution of [ $^3\text{H}$ ]pentamidine. No significant differences were observed in the [ $^{14}\text{C}$ ]sucrose-corrected uptake of [ $^3\text{H}$ ]pentamidine into brain regions, capillary depletion samples, or CVOs when D-eflornithine, L-eflornithine, or the racemic mixture were added to the artificial plasma ( $P > 0.05$  for each; data not shown).

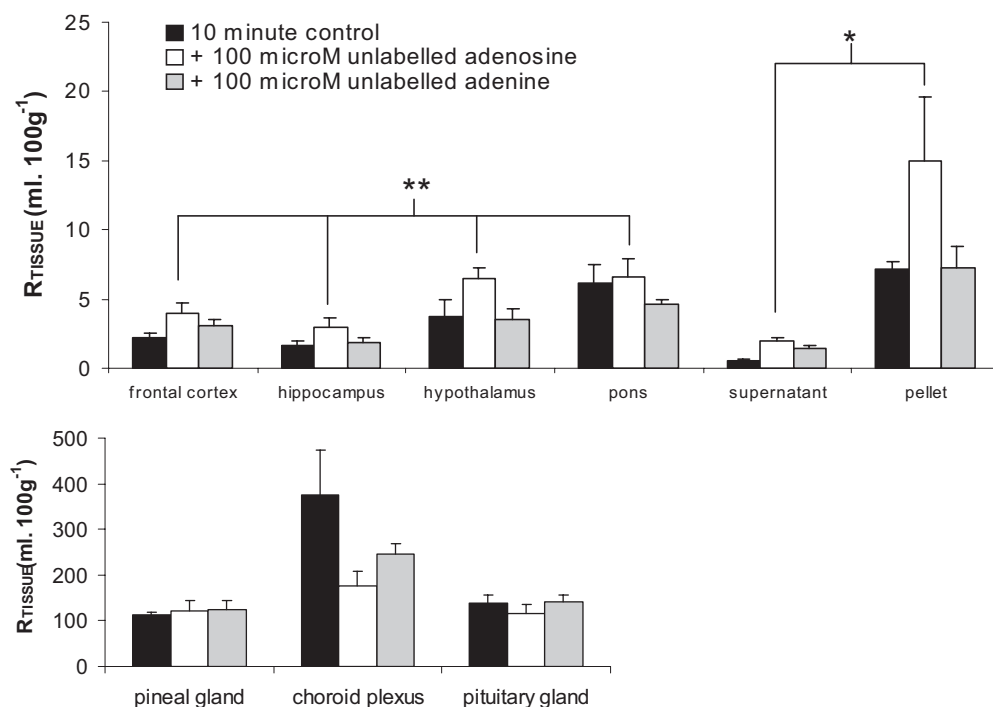


**Fig. 6.** [ $^{14}\text{C}$ ]Sucrose-corrected uptake of [ $^3\text{H}$ ]pentamidine in brain parenchyma and capillary depletion samples of mice that were perfused for 10 min with [ $^3\text{H}$ ]pentamidine in the absence and presence of 100  $\mu\text{M}$  adenosine or adenine. Each group represents  $n = 3-5$ . \*,  $P < 0.05$ ; \*\*,  $P < 0.001$  compared with controls.

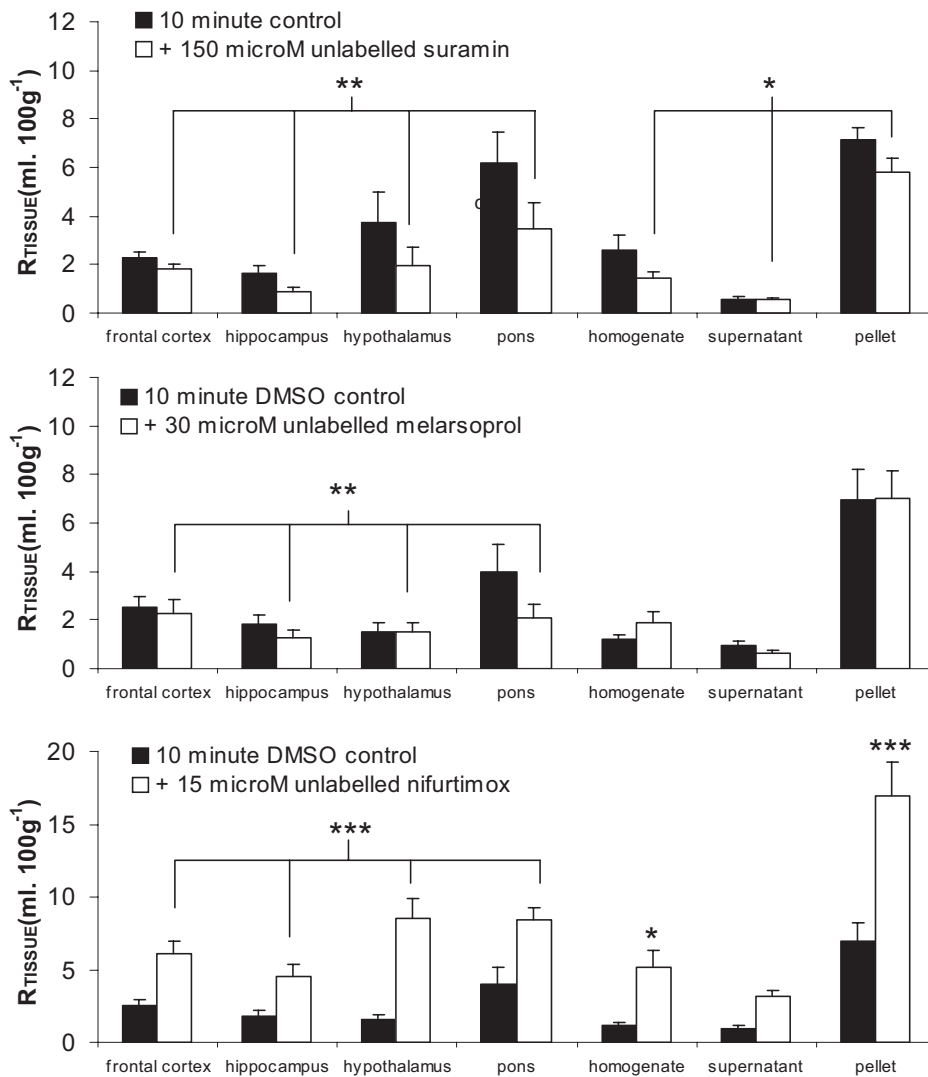


**Fig. 7.** The effect of unlabeled antitrypanosomal drugs on the [<sup>14</sup>C]sucrose-corrected uptake of [<sup>3</sup>H]pentamidine into brain and capillary depletion samples. Mice were perfused for 10 min with [<sup>3</sup>H]pentamidine, [<sup>14</sup>C]sucrose, and 100  $\mu$ M suramin, 30  $\mu$ M melarsoprol, or 15  $\mu$ M nifurtimox. Each group represents  $n = 3$  to 7. \*,  $P < 0.05$ ; \*\*,  $P < 0.01$ ; \*\*\*,  $P < 0.001$  compared with controls.

***T. brucei brucei* Infection and [<sup>3</sup>H]Pentamidine Uptake.** No significant differences were observed between the  $R_{\text{Tissue}}$  values of [<sup>14</sup>C]sucrose or [<sup>3</sup>H]pentamidine for all brain regions obtained from noninfected control mice compared with days 7, 14, and 21 p.i. In contrast, there was a significant increase in [<sup>14</sup>C]sucrose space at days 28 ( $P < 0.001$ ) and 35 ( $P = 0.020$ ) p.i. compared with noninfected control mice. This increase was greater at day 28 compared with day 35 p.i. ( $P = 0.049$ ). There was also an increase in [<sup>3</sup>H]pentamidine at day 28 ( $P < 0.001$ ) and day 35 ( $P < 0.001$ ) p.i. compared with noninfected control mice, but no significant difference between days 28 and 35 was observed for [<sup>3</sup>H]pentamidine ( $P > 0.05$ ; Fig. 8). An investigation into the extent of BBB breakdown at day 35 p.i. was also undertaken using [<sup>3</sup>H]suramin. Suramin (1429.2) has a considerably larger mol. wt. compared with [<sup>3</sup>H]pentamidine (340.4). There was a significant difference in the brain distribution of both [<sup>3</sup>H]suramin ( $P = 0.002$ ) and [<sup>14</sup>C]sucrose ( $P = 0.006$ ) between noninfected control and day 35 p.i. values (Table 1).

## Discussion

Pentamidine is not prescribed against stage 2 sleeping sickness because it is not thought to cross the BBB efficiently

enough to attain effective concentrations in the CNS (Rase-roka and Ormerod, 1986). This study indicates that intact [<sup>3</sup>H]pentamidine can cross both luminal and abluminal membranes of the BBB and be detected in the brain. However, analyses also revealed that [<sup>3</sup>H]pentamidine can be trapped by capillary endothelium. This has been observed for other diamidines (Sturk et al., 2004). A slow uptake of pentamidine into human brain also has been described, which might be a reflection of the trapping effect of the BBB, with it only being detectable  $\sim 30$  days after the start of a daily regimen ( $\sim 4$  mg/kg/day pentamidine isethionate) in AIDS patients (Donnelly et al., 1988). Furthermore, tissue and plasma protein binding of pentamidine is established and contributes to its long-lasting prophylactic effect in humans (Donnelly et al., 1988; Balasegaram et al., 2006) with pentamidine having a half-life of 22 to 47 h (Bronner et al., 1991). Pentamidine is not metabolized significantly in humans or mice (Waalkes et al., 1970), and this investigation supports this because we found no HPLC evidence of [<sup>3</sup>H]pentamidine being metabolized in brain tissue.

Pentamidine plasma concentrations in *T. brucei gambiense*-infected patients after the standard treatment for HAT (3.5–4.5 mg base/kg body weight) ranged from 0.042 to 0.230  $\mu$ M (Bronner et al., 1991). Thus, the [<sup>3</sup>H]pentamidine plasma



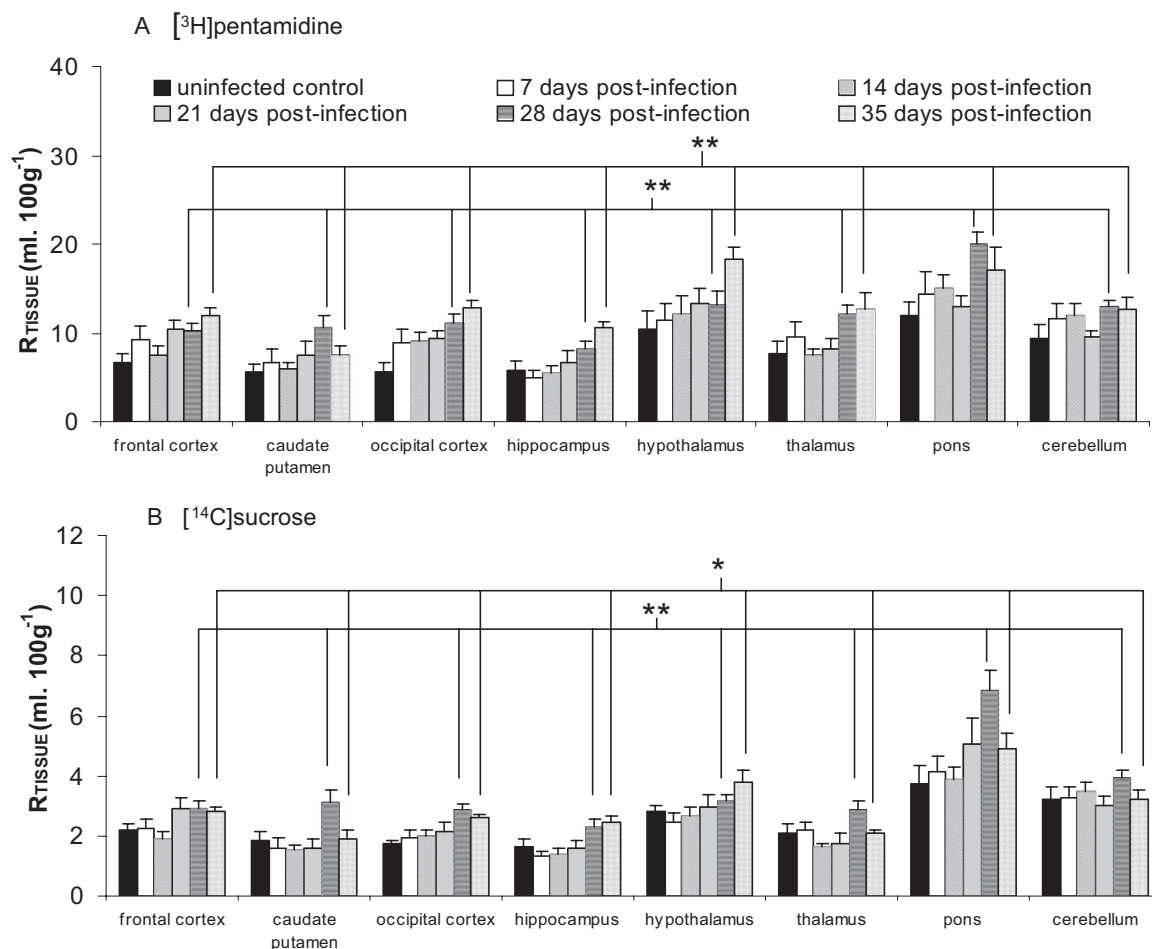


**Fig. 8.** Effect of *T. brucei brucei* infection on [<sup>3</sup>H]pentamidine and [<sup>14</sup>C]sucrose brain uptake. Trypanosome-infected BALB/c mice were perfused on days 7, 14, 21, 28, and 35 p.i. Infected were compared with noninfected mice: \*, *P* < 0.05; and \*\*, *P* < 0.001. Each group represents *n* = 5 to 7.

**TABLE 1**

Distribution of suramin into the frontal cortex of uninfected mice and mice 35 days p.i. with *T. brucei brucei*  
 Percentage increase in the brain distribution associated with infection is also reported. Each point, *n* = 4.

Drug	R <sub>Tissue</sub> (Uncorrected) Control	R <sub>Tissue</sub> (Uncorrected) Infected	Increase
	<i>ml · 100 g<sup>-1</sup></i>		<i>%</i>
[ <sup>3</sup> H]Suramin	1.5 ± 0.2	2.7 ± 0.4	88
[ <sup>14</sup> C]Sucrose	2.8 ± 0.3	4.0 ± 0.5	43

concentration of 0.1 μM used in this experimental study is within this range. Furthermore, we estimate that, after a 30-min perfusion with [<sup>3</sup>H]pentamidine, concentrations of [<sup>3</sup>H]pentamidine in the brain homogenate, supernatant (i.e., brain parenchyma in the absence of capillary endothelium), and pellet (i.e., capillary endothelium) were ~5, 2, and 15 nM or 0.013, 0.005, and 0.04% of administered dose, respectively. This suggests that pentamidine does not reach a concentration in the brain that would completely eradicate certain strains of cerebral parasites because the IC<sub>50</sub> value of pentamidine against different *T. brucei gambiense* isolates ranges from 1.8 to 26.1 nM (Likeufack et al., 2006). Although the criteria for the correct staging of HAT is debatable (Kennedy, 2006), successful pentamidine treatment of early second stage HAT patients with a CSF white cell count up to 20/μl and CSF trypanosomes has been reported (Doua et al., 1996;

Lejon et al., 2003). It is interesting that our study indicates that the pentamidine concentration achieved in the brain could be doubled by inhibiting P-gp efflux, suggesting that the success rate of pentamidine in treating this early late stage could be improved by combining with a P-gp inhibitor. However, it is possible that this would cause CNS side effects. The high [<sup>3</sup>H]pentamidine accumulation by the choroid plexuses (128 μM at 30 min) may contribute to the efficacy of pentamidine in this transition to a full CNS stage infection. This is because trypanosomes are detected at the early stage of infection in the choroid plexus, and it is thought that the CVOs provide a pathway for the trypanosomes to invade the CNS (Schultzberg et al., 1988).

Pentamidine is detectable in human CSF with concentrations of 1.7 to 3.9 nM corresponding to 0.5 to 0.8% of plasma concentration after HAT treatment (Bronner et al., 1991). The present study would also indicate that [<sup>3</sup>H]pentamidine can cross the blood-CSF barrier and reach CSF. The large [<sup>3</sup>H]pentamidine accumulation by the choroid plexus and the capillary endothelium is probably related to its two positive charges at pH 7.4 and the hydrophobic linker between the amidine groups that enable pentamidine to interact with negatively charged intracellular components.

Uncharged or weakly basic molecules are efficiently transported by P-gp and pentamidine is a basic drug, which is ionized at physiological pH. Using two strains of P-gp-defi-

cient mice, we found evidence that [ $^3\text{H}$ ]pentamidine can be removed from the CNS by P-gp as expressed by *mdr1a*. It is interesting that the *Mdr1a* P-gp is the major mouse P-gp and is the only P-gp in brain capillaries (Borst and Schinkel, 1997). We found no difference in the relative effect of removing *mdr1a* [i.e., CF1-*mdr1a*(+/+) versus CF1-*mdr1a*(-/-)] compared with removing *mdr1a* and *mdr1b* [i.e., FVB-*mdr1a/1b*(+/+) versus FVB-*mdr1a/1b*(-/-)] when examining [ $^3\text{H}$ ]pentamidine brain distribution, which further suggests the absence of BBB *mdr1b*, although it may be that pentamidine is not transported by *mdr1b*. In contrast, [ $^3\text{H}$ ]pentamidine distribution into the choroid plexus was not affected by the absence of either *mdr1a* or *mdr1a/mdr1b*. The endothelial cells of the human choroid plexus do not express P-gp, and *mdr1a* was not detected in the choroid plexus of FVB mice (Cordon-Cardo et al., 1989; Soontornmalai et al., 2006). This suggests that the major site of P-gp-dependent brain efflux is at the BBB and not the choroid plexus (Gazzin et al., 2008).

Further investigations using the FVB-*Mdr1a/1b*(-/-) mice provided evidence of pentamidine removal from the CNS by MRP. Multidrug transporters have overlapping substrate specificity for numerous hydrophobic compounds, and members of the MRP family are expressed at the blood-brain and blood-CSF barrier (Regina et al., 1998; Zhang et al., 2000; Soontornmalai et al., 2006). The functional importance of Mrp1 expressed at the BBB is controversial (Gazzin et al., 2008). Mrp4 and Mrp5, but not Mrp2 and Mrp3, are expressed in FVB murine cerebral capillaries (Soontornmalai et al., 2006) and are implicated in nucleoside analog removal from mammalian cells (Schuetz et al., 1999; Wijnholds et al., 2000). Thus, the increase in the brain distribution of [ $^3\text{H}$ ]pentamidine by the adenosine could be a consequence of interaction at Mrp4 and/or Mrp5, consistent with the apparent selectivity over adenine.

Mrp1 and Mrp3 (but not Mrp5) have been identified in the choroid plexus epithelium taken from FVB mice (Soontornmalai et al., 2006). Mrp1 is expressed at the basolateral face of the human choroid plexus (Rao et al., 1999), and the choroid plexus is the main site of blood-facing, Mrp1-dependent cellular efflux from the rat brain (Gazzin et al., 2008). In our study, indomethacin increased [ $^3\text{H}$ ]pentamidine accumulation by the choroid plexus of FVB-*mdr1a/mdr1b*(-/-) mice consistent with [ $^3\text{H}$ ]pentamidine removal by Mrp1. Cross-competition studies revealed that nifurtimox increased [ $^3\text{H}$ ]pentamidine distribution to the brain, but not to the CVOs, providing evidence of interaction with an efflux transporter (possibly P-gp or MRP) shared by the two trypanocides.

Further studies revealed melarsoprol and pentamidine could interact at an influx transporter at the BBB and was not affected by adenosine or adenine. It is interesting that although the P2/adenosine-sensitive pentamidine transporter is important for the trypanosome uptake of pentamidine and melarsoprol (Carter and Fairlamb, 1993), melarsoprol uptake is also attributable to another transporter, possibly high-affinity pentamidine transporter 1 (Bridges et al., 2007). It is clear that pentamidine and melarsoprol share a structural motif to allow joint recognition by transporters. Taken together with the self-inhibition data, this interaction of pentamidine with an influx transporter indicates that pentamidine is more sensitive to the efflux transporter compared with the influx transporter.

Suramin reduced the uptake of [ $^3\text{H}$ ]pentamidine into the brain, but based on previous studies (Sanderson et al., 2007), it is unlikely to be due to a transporter. It may be that the positively charged pentamidine interacts with the negatively charged suramin (Pépin and Khonde, 1996). This pentamidine-suramin complex, like suramin alone, cannot cross the BBB (Sanderson et al., 2007). There was no evidence of eflornithine affecting [ $^3\text{H}$ ]pentamidine CNS distribution.

The murine model of HAT revealed an absence of BBB changes early (up to day 21 p.i.) in the course of infection; however, there was widespread breakdown of BBB integrity from day 28 p.i. This caused a significant increase in the accumulation of [ $^3\text{H}$ ]pentamidine (mol. wt. 340) and [ $^{14}\text{C}$ ]sucrose (mol. wt. 342) into the brain regions at days 28 and 35 p.i. compared with results from noninfected controls and days 7, 14, and 21 p.i. mice. An investigation into the effects of infection on [ $^3\text{H}$ ]suramin distribution revealed that large molecules (mol. wt. 1429) were able to cross the BBB at 35 days p.i. This clearly illustrates the extent of BBB damage associated with late trypanosome infection.

Pentamidine is able to cross the BBB, but a proportion is retained within the capillary endothelium. This may well explain its inability to treat well established CNS trypanosome infection. Furthermore, pentamidine movement into the CNS is a complex process involving multiple transporters. Trypanosome infection did not alter the BBB passage of [ $^3\text{H}$ ]pentamidine until the end stage of infection. There was no effect on the CNS distribution of [ $^3\text{H}$ ]pentamidine upon the addition of eflornithine. However, therapy combining pentamidine with the other antitrypanosomal agents, nifurtimox, suramin, and melarsoprol, is likely to affect the final drug concentrations achieved within the CNS. This may have serious consequences if it leads to subtherapeutic concentrations being achieved locally. Not only would this fail to clear the infection from the brain, leading to relapse with late-stage HAT, but it could potentially lead to the development of drug resistance as a result of selection pressures placed on the parasite population within the CNS. The interaction of [ $^3\text{H}$ ]pentamidine with P-gp and MRP suggests that a possible strategy to improve the CNS delivery of pentamidine, and possibly other diamidines under therapeutic consideration, would be to combine the drugs with a P-gp or MRP inhibitor. A transporter-specific inhibitor would be the recommended approach as the less selective inhibitors, which inhibit multiple transporters, leave the brain more susceptible to damage by putative toxins and consequently adverse effects (Varatharajan and Thomas, 2009).

## References

- Balasegaram M, Harris S, Checchi F, Hamel C, and Karunakara U (2006) Treatment outcomes and risk factors for relapse in patients with early-stage human African trypanosomiasis (HAT) in the Republic of the Congo. *Bull World Health Organ* **84**:777–782.
- Basselin M, Denise H, Coombs GH, and Barrett MP (2002) Resistance to pentamidine in *Leishmania mexicana* involves exclusion of the drug from the mitochondrion. *Antimicrob Agents Chemother* **46**:3731–3738.
- Berger BJ, Reddy VV, Le ST, Lombardy RJ, Hall JE, and Tidwell RR (1991) Hydroxylation of pentamidine by rat liver microsomes. *J Pharmacol Exp Ther* **256**:883–889.
- Borst P and Schinkel AH (1997) Genetic dissection of the function of mammalian P-glycoproteins. *Trends Genet* **13**:217–222.
- Bridges DJ, Gould MK, Nerima B, Mäser P, Burchmore RJ, and de Koning HP (2007) Loss of the high-affinity pentamidine transporter is responsible for high levels of cross-resistance between arsenical and diamidine drugs in African trypanosomes. *Mol Pharmacol* **71**:1098–1108.
- Bronner U, Doua F, Ericsson O, Gustafsson LL, Miézan TW, Rais M, and Rombo L (1991) Pentamidine concentrations in plasma, whole blood and cerebrospinal fluid

- during treatment of *Trypanosoma gambiense* infection in Cote d'Ivoire. *Trans R Soc Trop Med Hyg* **85**:608–611.
- Burri C and Brun R (2003) Eflornithine for the treatment of human African trypanosomiasis. *Parasitol Res* **90** (Suppl 1):S49–S52.
- Carter NS and Fairlamb AH (1993) Arsenical-resistant trypanosomes lack an unusual adenosine transporter. *Nature* **361**:173–176.
- Coelho AC, Beverley SM, and Cotrim PC (2003) Functional genetic identification of PRP1, an ABC transporter superfamily member conferring pentamidine resistance in *Leishmania major*. *Mol Biochem Parasitol* **130**:83–90.
- Cordon-Cardo C, O'Brien JP, Casals D, Rittman-Grauer L, Biedler JL, Melamed MR, and Bertino JR (1989) Multidrug-resistance gene (P-glycoprotein) is expressed by endothelial cells at blood-brain barrier sites. *Proc Natl Acad Sci U S A* **86**:695–698.
- de Koning HP (2001) Transporters in African trypanosomes: role in drug action and resistance. *Int J Parasitol* **31**:512–522.
- Donnelly H, Bernard EM, Rothkotter H, Gold JW, and Armstrong D (1988) Distribution of pentamidine in patients with AIDS. *J Infect Dis* **157**:985–989.
- Doua F, Miezian TW, Sanon Singaro JR, Boa Yapo F, and Baltz T (1996) The efficacy of pentamidine in the treatment of early-late stage *Trypanosoma brucei gambiense* trypanosomiasis. *Am J Trop Med Hyg* **55**:586–588.
- Gazzin S, Strazielle N, Schmitt C, Fevre-Montange M, Ostrow JD, Tiribelli C, and Ghersi-Egea JF (2008) Differential expression of the multidrug resistance-related proteins ABCB1 and ABCG1 between blood-brain interfaces. *J Comp Neurol* **510**:497–507.
- González-Martin G, Thambo S, Paulos C, Vásquez I, and Paredes J (1992) The pharmacokinetics of nifurtimox in chronic renal failure. *Eur J Clin Pharmacol* **42**:671–673.
- Huai-Yun H, Secrest DT, Mark KS, Carney D, Brandquist C, Elmquist WF, and Miller DW (1998) Expression of multidrug resistance-associated protein (MRP) in brain microvessel endothelial cells. *Biochem Biophys Res Commun* **243**:816–820.
- Kennedy PG (2006) Diagnostic and neuropathogenesis issues in human African trypanosomiasis. *Int J Parasitol* **36**:505–512.
- Lejon V, Legros D, Savignoni A, Etegegorry MG, Mbulamberi D, and Büscher P (2003) Neuro-inflammatory risk factors for treatment failure in "early second stage" sleeping sickness patients treated with pentamidine. *J Neuroimmunol* **144**:132–138.
- Leprohon P, Légaré D, Girard I, Papadopoulou B, and Ouellette M (2006) Modulation of *Leishmania* ABC protein gene expression through life stages and among drug-resistant parasites. *Eukaryot Cell* **5**:1713–1725.
- Likeufack AC, Brun R, Fomena A, and Truc P (2006) Comparison of the in vitro drug sensitivity of *Trypanosoma brucei gambiense* strains from West and Central Africa isolated in the periods 1960–1995 and 1999–2004. *Acta Trop* **100**:11–16.
- Milord F, Loko L, Ethier L, Mpia B, and Pépin J (1993) Eflornithine concentrations in serum and cerebrospinal fluid of 63 patients treated for *Trypanosoma brucei gambiense* sleeping sickness. *Trans R Soc Trop Med Hyg* **87**:473–477.
- Murakami H, Ohkura A, Takanaga H, Matsuo H, Koyabu N, Naito M, Tsuruo T, Ohtani H, and Sawada Y (2005) Functional characterization of adenosine transport across the BBB in mice. *Int J Pharm* **290**:37–44.
- Neuwelt E, Abbott NJ, Abrey L, Banks WA, Blakley B, Davis T, Engelhardt B, Grammas P, Nedergaard M, Nutt J, et al. (2008) Strategies to advance translational research into brain barriers. *Lancet Neurol* **7**:84–96.
- Pépin J and Khonde N (1996) Relapses following treatment of early-stage *Trypanosoma brucei gambiense* sleeping sickness with a combination of pentamidine and suramin. *Trans R Soc Trop Med Hyg* **90**:183–186.
- Priotto G, Kasparian S, Nguoua D, Ghorashian S, Arnold U, Ghabri S, and Karunakara U (2007) Nifurtimox-eflornithine combination therapy for second-stage *Trypanosoma brucei gambiense* sleeping sickness: a randomized clinical trial in Congo. *Clin Infect Dis* **45**:1435–1442.
- Rao VV, Dahlheimer JL, Bardgett ME, Snyder AZ, Finch RA, Sartorelli AC, and Piwnicka-Worms D (1999) Choroid plexus epithelial expression of MDR1 P-glycoprotein and multidrug resistance-associated protein contribute to the blood-cerebrospinal-fluid drug-permeability barrier. *Proc Natl Acad Sci U S A* **96**:3900–3905.
- Raseroka BH and Ormerod WE (1986) The trypanocidal effect of drugs in different parts of the brain. *Trans R Soc Trop Med Hyg* **80**:634–641.
- Regina A, Koman A, Piciotti M, El Hafny B, Center MS, Bergmann R, Couraud PO, and Roux F (1998) Mrp1 multidrug resistance-associated protein and P-glycoprotein expression in rat brain microvessel endothelial cells. *J Neurochem* **71**:705–715.
- Sanderson L, Dogruel M, Rodgers J, Bradley B, and Thomas SA (2008) The blood-brain barrier significantly limits eflornithine entry into *Trypanosoma brucei brucei* infected mouse brain. *J Neurochem* **107**:1136–1146.
- Sanderson L, Khan A, and Thomas S (2007) Distribution of suramin, an antitrypanosomal drug, across the blood-brain and blood-cerebrospinal fluid interfaces in wild-type and P-glycoprotein transporter-deficient mice. *Antimicrob Agents Chemother* **51**:3136–3146.
- Schuetz JD, Connelly MC, Sun D, Paibr SG, Flynn PM, Srinivas RV, Kumar A, and Fridland A (1999) MRP4: A previously unidentified factor in resistance to nucleoside-based antiviral drugs. *Nat Med* **5**:1048–1051.
- Schultzberg M, Ambatsis M, Samuelsson EB, Kristensson K, and van Meirvenne N (1988) Spread of *Trypanosoma brucei* to the nervous system: early attack on circumventricular organs and sensory ganglia. *J Neurosci Res* **21**:56–61.
- Soontrammalai A, Vlaming ML, and Fritschy JM (2006) Differential, strain-specific cellular and subcellular distribution of multidrug transporters in murine choroid plexus and blood-brain barrier. *Neuroscience* **138**:159–169.
- Sturk LM, Brock JL, Bagnell CR, Hall JE, and Tidwell RR (2004) Distribution and quantitation of the anti-trypanosomal diamidine 2,5-bis(4-amidinophenyl)furan (DB75) and its *N*-methoxy prodrug DB289 in murine brain tissue. *Acta Trop* **91**:131–143.
- Varatharajan L and Thomas SA (2009) The transport of anti-HIV drugs across blood-CNS interfaces: summary of current knowledge and recommendations for further research. *Antiviral Res* doi:10.1016/j.antiviral.2008.12.013.
- Waalkes TP, Denham C, and DeVita VT (1970) Pentamidine: clinical pharmacologic correlations in man and mice. *Clin Pharmacol Ther* **11**:505–512.
- Waalkes TP and DeVita VT (1970) The determination of pentamidine (4,4'-diamidinophenoxy-pentane) in plasma, urine, and tissues. *J Lab Clin Med* **75**:871–878.
- Wijnholds J, Mol CA, van Deemter L, de Haas M, Scheffer GL, Baas F, Beijnen JH, Scheper RJ, Hatse S, De Clercq E, et al. (2000) Multidrug-resistance protein 5 is a multispecific organic anion transporter able to transport nucleotide analogs. *Proc Natl Acad Sci U S A* **97**:7476–7481.
- Williams SA, Abbruscato TJ, Hrubby VJ, and Davis TP (1996) Passage of a delta-opioid receptor selective enkephalin, [D-penicillamine2,5] enkephalin, across the blood-brain and the blood-cerebrospinal fluid barriers. *J Neurochem* **66**:1289–1299.
- Zhang Y, Han H, Elmquist WF, and Miller DW (2000) Expression of various multidrug resistance-associated protein (MRP) homologues in brain microvessel endothelial cells. *Brain Res* **876**:148–153.

**Address correspondence to:** Dr. Sarah Ann Thomas, King's College London, Pharmaceutical Sciences Research Division, Hodgkin Building, Guy's Campus, London, SE1 1UL, UK. E-mail: sarah.thomas@kcl.ac.uk